IOPscience iopscience.iop.org

Home Search Collections Journals About Contact us My IOPscience

Photolithography on bulk micromachined substrates

This article has been downloaded from IOPscience. Please scroll down to see the full text article.

2009 J. Micromech. Microeng. 19 055005

(http://iopscience.iop.org/0960-1317/19/5/055005)

View the table of contents for this issue, or go to the journal homepage for more

Download details:
IP Address: 131.180.130.109
The article was downloaded on 08/08/2011 at 10:24

Please note that terms and conditions apply.

J. Micromech. Microeng. **19** (2009) 055005 (6pp) doi:10.1088/0960-1317/19/5/055005

Photolithography on bulk micromachined substrates

W J Venstra[1,2], J W Spronck[2], P M Sarro[3] and J van Eijk[2]

[1] Kavli Institute of Nanoscience, Lorentzweg 1, 2628CJ Delft, The Netherlands
[2] Precision and Microsystems Engineering, Mekelweg 2, 2628CD Delft, The Netherlands
[3] DIMES, Electronic Components, Technology and Materials Laboratory, Feldmannweg 17, 2628CT Delft, The Netherlands

E-mail: w.j.venstra@tudelft.nl

Received 20 February 2009, in final form 17 March 2009
Published 15 April 2009
Online at stacks.iop.org/JMM/19/055005

Abstract
Photolithography on high topography substrates, such as the sidewalls or the bottom of cavities and trenches created by bulk micromachining, enables the design of complex three-dimensional structures. When a contact lithography system is used to pattern such substrates, local gaps exist between the mask and the substrate. In this paper we investigate the deformation of patterns as a result of these local gaps. We determine the position accuracy and the minimum size of features that can be patterned as a function of the gap distance. Deformations introduced by the optical system are quantified for a common exposure tool, and compared to pattern deformation due to variations in photoresist layer thickness. Finally, methods to improve the quality of patterns transferred through gaps up to 350 μm are discussed.

(Some figures in this article are in colour only in the electronic version)

1. Introduction

The patterning of bulk micromachined substrates enables the fabrication of complex three-dimensional structures in silicon wafers and other substrates. For instance, conductors can be patterned inside fluid channels for electrophoresis, to heat the fluid, or to direct electro osmotic flow [1]. Another application is the fabrication of photo detectors on the bottom of reaction chambers for fluorescence measurements or to monitor cell growth processes [2, 3]. Pattern transfer on high topographies can also be used to package mechanical structures which operate in fluids, such as cantilever sensors. Clearance is required for the cantilever to move freely through the liquid. For this purpose, cavities can be created in the cover plate as shown in figure 1(*a*). Alternatively, the device can be fabricated in a single layer, when the cantilever is formed in slanted or recessed membranes [4–8], as is shown in figures 1(*b*), (*c*), respectively. The fabrication effort is reduced, as only one substrate is processed and a flat cover can be used without any alignment. Figure 1(*d*) shows the realization of such a device: two 300 μm long v-shaped silicon nitride cantilevers are suspended deep inside a fluid well, 100 μm below the wafer surface. This configuration can be used for individual functionalization of the cantilever sensors [9].

Pattern transfer on high topography substrates starts with a conformal layer of photoresist. Several techniques have been developed to coat bulk micromachined substrates, including a modified spin coating technique [10], spray coating [11–13] and electrochemical deposition [14–16]. Contact lithography is a straightforward technique to fabricate devices with critical dimensions down to several micrometers. On high topography substrates however, a gap is present between the mask and the substrate and contact is lost: the mask pattern is projected through the gap onto the substrate. Inside the gap, the pattern is deformed. In this paper, we study the origins of these deformations by measuring the shape of the patterns as a function of the gap distance. We quantify the errors introduced by the exposure system, compare them to the deformations resulting from a non-uniform photoresist layer thickness, and where possible suggest measures to reduce them.

2. Fabrication

The variation in shape of projected patterns as a function of the distance between the mask and the substrate is measured.

 © 2009 IOP Publishing Ltd Printed in the UK

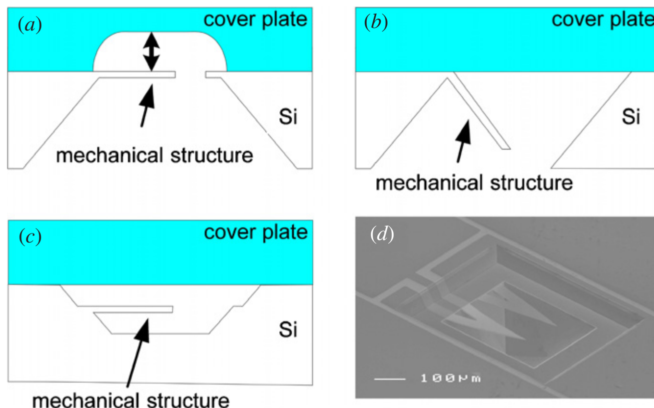

Figure 1. Packaging of a freely moving mechanical structure in a silicon wafer. (*a*) Clearance is provided by the cavity in the cover plate. (*b*) and (*c*) A flat cover can be used when the mechanical structure is patterned on slanted or recessed planes. (*d*) Scanning electron microscope (SEM) image of a pair of cantilevers realized according to (*c*).

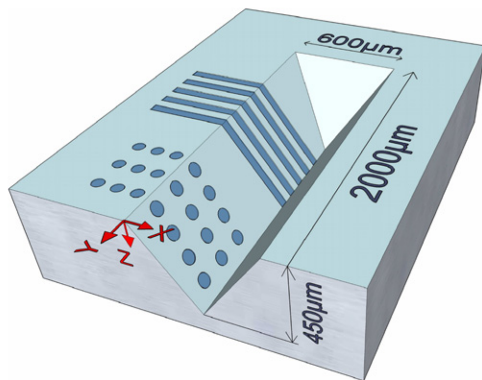

Figure 2. Sketch of dots and lines, projected on the sidewalls of a 450 μm deep v-shaped cavity. The dot diameter varies between 1 and 100 μm, and the distance between the mask and the substrate, the gap distance z, equals 50, 150, 250 and 350 μm. The x-coordinate marks the position of the pattern relative to the edge of the cavity, and y is the relative position of the feature along the long edge of the cavity.

A varying gap is created by etching deep v-shaped cavities in 4' (1 0 0) silicon wafers. A potassium hydroxide (KOH) solution is used which results in a cavity sidewall at an angle of 54.7° with respect to the wafer surface. The dimensions of the cavities are 2000 μm × 600 μm, and the gap between the mask and the substrate, i.e. the cavity depth, ranges from zero to 450 μm. An Electronic Visions Group EVG101 spray coating system is used to coat the wafers with a uniform layer of photoresist. A positive resist is used, Clariant AZ4562, and the thickness of the deposited layer was 5–8 μm. After baking the photoresist, the mask is applied and the wafers are exposed in an Electronic Visions Group EV420 contact alignment and exposure tool using a near-UV source (λ = 350–450 nm) at 625 mJ cm^{-2}.

Patterns of lines and dots are projected on the slanted substrate plane. Figure 2 shows the experiment schematically. Groups of five equally spaced identical lines are patterned, with a line width varying between 1 μm and 100 μm. Dots with a diameter range between 10 and 100 μm are projected at a depth of 50, 150, 250 and 350 μm. After development of the photoresist, the dimensions and position of the resulting patterns are measured and related to their nominal value.

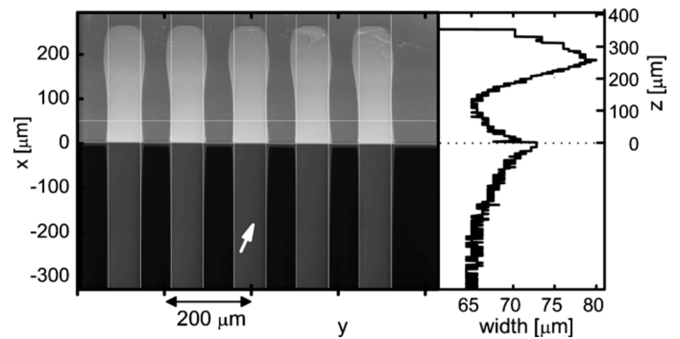

Figure 3. SEM image of a line array with detected cavity edge and line edges, and measurement of the width of the line indicated by the arrow.

3. Measurements

The patterns are measured using a Philips SEM525M scanning electron microscope (SEM). The electron beam is focused at $z \approx 225$ μm, and 1024 × 768 pixels × 8 bits images were acquired using 16× averaging at 10 μs averaging time. The dimensions of the dot patterns are measured using Soft-Imaging image analysis software. The line patterns are measured using a custom algorithm written in Matlab. First the position of the long edge of the cavity is detected, to determine the starting location of the gap. From the angle of the cavity, 54.7°, the gap distance z is calculated. The position of the lines is detected by transitions in the gray scale value. Figure 3 shows a SEM image of five 65 μm wide lines, with the detected transitions in the gray scale value across a horizontal line at position $x = 50$ μm. The width of the line indicated by the arrow in the figure is plot as a function of its position x and the gap distance, z. The resolution of the measurement is 1 pixel, which corresponds to approximately 0.5 μm. No interpolation was used and the measurements obtained using the algorithm were in good agreement with the measurements using the Soft-Imaging software. We investigated the effect of through-focus rotation of the SEM image, due to spiraling motion of the electrons through the column [17]. The rotation induced by the SEM when moving through focus over a distance of 500 μm was found to be negligible compared to the effects we investigate in the following section.

4. Results and discussion

Measurement of the pattern size and position as a function of the gap distance suggests the presence of four major effects, which are individually addressed here.

4.1. Divergence

First, the position of the center of the lines is measured as a function of the gap distance, z. Lines running through the center of the cavity are measured, as to exclude effects of

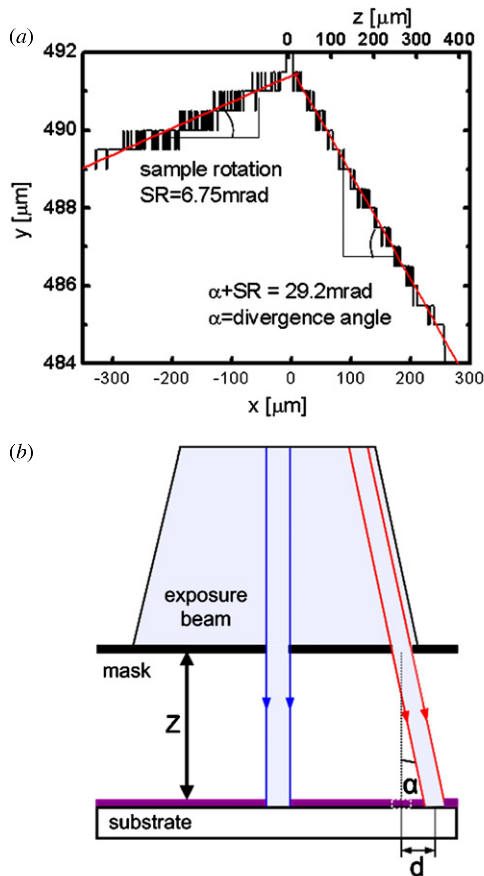

Figure 4. (*a*) Measurement of the center position of a single line as a function of the coordinate along the line. The constant angle marked SR, at $x < 0$ (which corresponds to $z = 0$), represents the rotation between the sample and the figure axes. The position of the line for $x > 0$ is shifted by the divergence of the exposure beam, α. (*b*) Schematic representation of the exposure beam, the mask and the substrate. Divergence is zero near the optical axis, off-axis the angle is α.

photoresist thickness variations along the cavity as will be described in section 4.3. Figure 4(*a*) shows the measured position of the center of one such line as a function of the coordinate along the line, x. The gap distance, z, is indicated by the top horizontal axis. The constant angle marked SR in the figure represents the rotation between the sample and the figure axes. At the cavity edge, $x = 0$, the angle changes to a new value marked α + SR in the figure. The angle α is attributed to the divergence of the exposure beam, as will be explained below.

Figure 4(*b*) schematically shows the exposure beam with the mask and the substrate. Due to the diverging exposure beam the projection is shifted by a distance d, equal to the divergence angle, α, times the gap distance z. The effect is large outside the optical axis of the exposure system, and negligible for small gaps and near the optical axis. It is noted that the effect in figure 3(*a*) is measured in a cavity located near the edge of the wafer, where the effect is maximal. In this region, values between 18 and 35 mrad are found, which is close to the maximum specified for this exposure system [18]. Beam divergence has a considerable effect on the position accuracy of lines transferred on deep recessed substrates. This

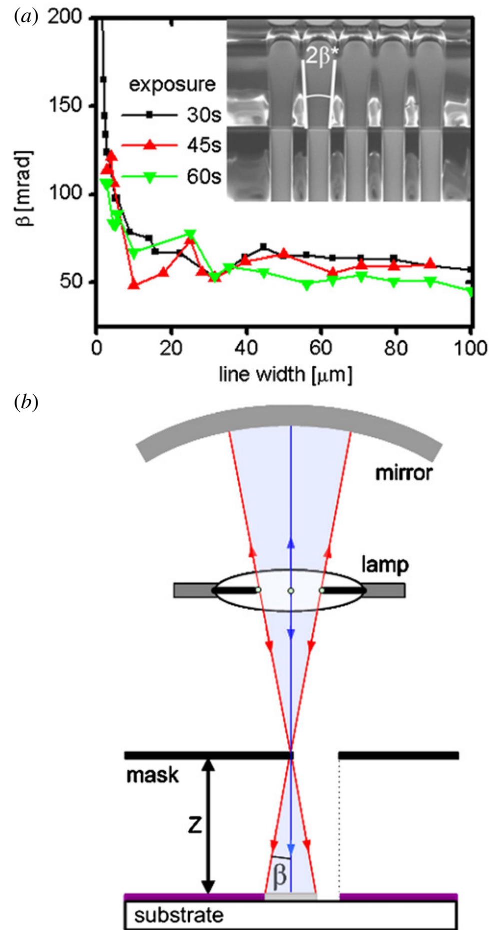

Figure 5. (*a*) Measured angle β as a function of the line width. The inset shows a SEM of the developed photoresist. The angle $2\beta^*$, indicated by the white lines, equals the angle 2β projected on the xy-plane. (*b*) Schematic overview of the exposure system including rays emitted from the center and the endpoints of the lamp arc. The edge of the projected feature is poorly defined, as indicated by the gray area.

exposure system introduces a lateral position error up to 10 μm in patterns projected at 250 μm depth.

4.2. Lamp dimensions

Figure 5(*a*), inset, shows a SEM image of the developed photoresist. From the edges of the partly removed resist, indicated by the white lines in the SEM image, it is clear that the exposed area increases with the gap distance. The exposed width is found to increase proportionally with the gap distance z. The main figure shows the measured angle β as a function of the nominal line width. The angle was measured for the same lines, exposed at three different doses (30 s, 45 s and 60 s exposure time). The angle depends neither on the line width nor on the exposure dose for nominal line widths down to 15 μm. We also note a rapid increase of the angle for line widths smaller than 15 μm.

The broadening of lines is attributed to the finite dimensions of the light source. Figure 5(*b*) shows the schematized optical path. By following rays from the edges of the lamp arc, the mask feature is effectively exposed at an angle

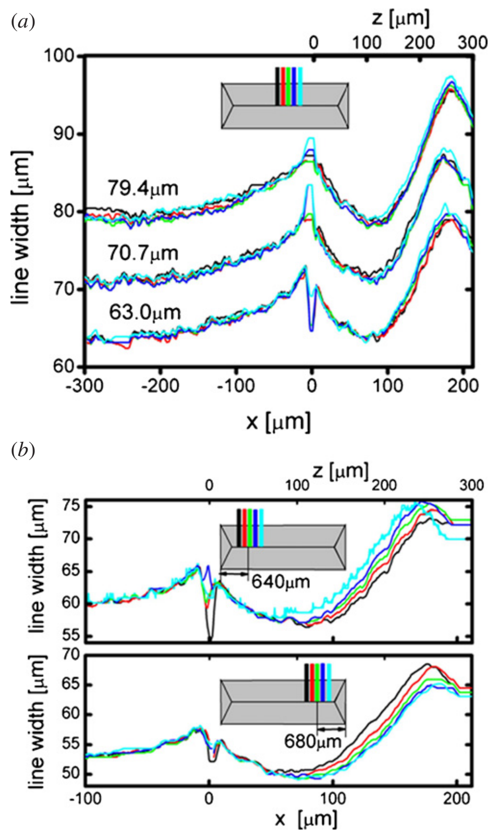

Figure 6. (*a*) Measured width of five lines through the center of the cavity, with nominal line width as indicated. (*b*) Line width measurements for five lines patterned close to the short edge of the cavity.

β. As a result, near the edge of the feature the masked area is exposed, albeit at a lower dose. Near the edge of the feature in the open area, the exposure dose is lower. As a consequence, the edges of the pattern are less well defined in the resist, and the final line width depends highly on the exposure dose. When the dose is increased, the lines become wider, until the outer boundaries given by the angle β are reached. In this limit, the patterned line width increases proportionally with the gap distance. The measurements in figure 5(*a*) suggest the same, as the broadening angle is independent of the nominal line dimensions. In our case a fixed angle β = 50–75 mrad is measured. At sufficient exposure, lines patterned at $z = 250$ μm are wider by as much as 25–40 μm as a result. The rapid increase in angle for narrow lines, is attributed to interference. These geometry-dependent effects are not further discussed here.

4.3. Variations in photoresist thickness

Spray coating is known to yield variations in the thickness of the deposited layer across sharp edges of etched cavities [16]. We investigate the results of a nonuniform photoresist layer by measuring the line patterns transferred in silicon nitride. After development and post-baking of the photoresist, the underlaying layer of silicon nitride is etched in a reactive ion etching system. The resist is removed, the lines in the silicon nitride are measured. Figure 6(*a*) shows three measurements on arrays of five lines with a nominal line width 63.0 μm, 70.7 μm and 79.4 μm. The line array is centered with respect to the cavity, as is shown in the inset. On the flat part of the wafer, position $x < 0$, we observe an increase in line width while approaching the cavity. On the slanted (1 1 1) plane there is a large variation, with a maximum and a minimum in the line width. These line width measurements reproduced well for cavities on different locations on the wafer.

We explain these observations qualitatively by taking into account variations in photoresist thickness. Since the resist is deposited in the liquid phase, once deposited it minimizes its surface area. As a result, resist is pulled into concave corners, e.g. the bottom of the cavity. In contrast, convex edges such as the cavity edge, are covered by a thinner layer [16]. From figure 6, the presence of the convex edge of the cavity influences the line width as from a distance of 200 μm, on the flat part of the wafer where $z = 0$. The line width increases until the edge is reached, which indicates a gradual decrease of the photoresist thickness. The same effect is visible on the slanted plane. The line width reduces again while moving away from the cavity edge. At a distance of approximately 180 μm from the edge, measured along the slanted plane, the nominal line width is recovered. The effect of lamp dimensions, discussed in section 4.2, becomes significant as from $z \approx 100$ μm. As a result, lines become wider until a maximum width is reached at $z = 250$ μm. Beyond this value, a reduction in width is observed. This effect is attributed to a gradual increase in photoresist thickness as the concave edge at the bottom of the cavity is approached. At a depth of 300 μm the line width reduces to zero.

We have also measured the line widths as a function of the *y*-coordinate, along the long edge of the cavity. Figure 6(*b*) shows measurements on arrays of lines placed near the edges of the cavity. The insets show the position of the line arrays with respect to the cavity. In contrast to 6(*a*), in 6(*b*) the line width curves disperse with the *y*-coordinate: the width decreases when approaching the short edge of the cavity. This suggests that the resist not only collects at the bottom of cavity, but also in the concave edges formed by the intersection of the (1 1 1) planes which form the cavity sidewalls. From this observation we conclude that surface tension is the main mechanism which introduces the variations in photoresist thickness, and the resulting deformation of patterns.

4.4. Exposure dose

Due to the nonzero lamp dimensions, described in section 4.2, the exposed area increases with the distance z between the mask and the substrate. As a result, the effective dose at the edges of features is lower. The size of deep transferred features is therefore highly dependent on the exposure dose. We exposed dots at different gaps and exposure times. For $z = 50$ μm the effects were not significant. Figure 7 shows the results for $z = 150$ μm, $z = 350$ μm. The exposure times were 45 s, 60 s, 90 s and 155 s.

The measurements confirm that small features are highly magnified when sufficiently exposed. In figure 7(*a*), the small dots are slightly demagnified in all cases except for the highest

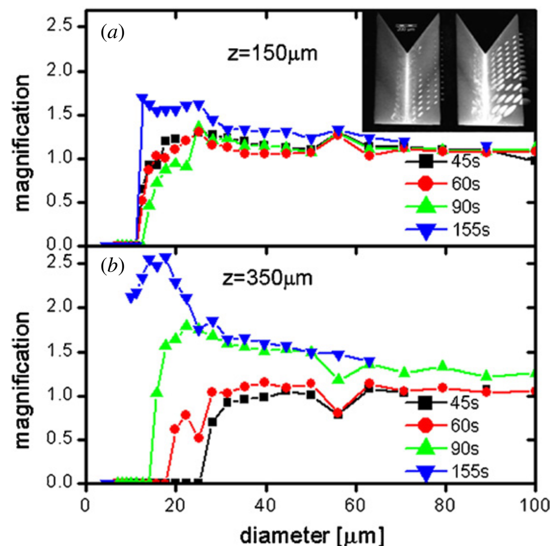

Figure 7. Magnification of dots on the cavity sidewall for different exposure doses at a gap of 150 μm (*a*) and 350 μm (*b*). The inset shows a tilted SEM image of a dot pattern.

dose. The measurements in figure 7(*b*) confirm the influence of the light source dimensions. At a distance of 350 μm, the diameter of the exposed area through a 20 μm feature is up to 2.6 times the nominal value. This confirms the magnification angle by the lamp dimensions, which was found to be 50–75 mrad in section 4.2. This corresponds to the blue line in figure 7(*b*), which represents the highest exposure dose.

As with the line width measurements, for all dot diameters the magnification was maximal at $z = 250$ μm. This enables the patterning of small (down to 10 μm) features to this depth. A locally reduced photoresist layer is expected in this area. For shallow cavities, up to a depth of 50 μm, features between 5 and 10 μm can be successfully transferred regardless of the exposure time.

5. Conclusions

We have studied the origins of the distortion of patterns transferred over high topography substrates using a contact lithography system. The position and size of test patterns were measured as a function of the gap distance between the mask and the substrate. These deformations were reproducibly quantified for an Electronic Visions Group EVG420 exposure system. It is found that divergence of the light source results in inaccurate position of transferred patterns, and that the nonzero lamp dimensions affect the size of the transferred pattern. The inaccuracy in position and size are comparable with the pattern deformation caused by a non-uniform photoresist layer, when a spray coat system is used. The effects of divergence and lamp dimensions are independent of the design geometry, and therefore it should be possible to compensate the errors by an appropriate transformation of the mask coordinates, as a function of the gap distance and the location with respect to the optical axis of the exposure system. A more effective solution is to reduce the dimensions of the light source in the exposure tool. As for the variations in photoresist thickness, we observed that convex edges are covered by a thinner layer, and resist is pulled into concave edges. This results in deformed patterns. These effects are not only present in the gap but also at hundreds of micrometers distance from the gap, on the flat area of the wafer where the gap is zero. The present work demonstrates that accurate transfer of patterns on high topography substrates requires not only a uniform photoresist layer. The exposure tool introduces significant deformations in the gap. Quantitative results will depend on the particular exposure system, but the same effects can be quantified for other photolithography systems using the techniques described in this paper.

Acknowledgments

The authors thank Urs Staufer for valuable discussions, the DIMES IC Process group for technical support and Dr Nga Pham for suggestions with respect to spray coating of photoresist. Financial support from the Delft Center for Mechatronics and Microsystems, and NWO (VICI) is acknowledged.

References

[1] Stroock A D, Weck M, Chiu D T, Huck W T S, Kenis P J A, Ismagilov R F and Whitesides G M 2000 Patterning electro-osmotic flow with patterned surface charge *Phys. Rev. Lett.* **84** 3314

[2] Young I T *et al* 2003 Monitoring enzymatic reactions in nanolitre wells *J. Microsc.* **212** 254–63

[3] Bao N, Wang J and C Lu 2008 Recent advances in electric analysis of cells in microfluidic systems *Anal. Bioanal. Chem.* **391** 933–42

[4] Oosterbroek R E, Berenschot J W, Schlautmann S, Krijnen G J M, Lammerink T S J, Elwenspoek M C and Van den Berg A 1999 Designing, simulation and realization of in-plane operating micro valves, using new etching techniques *J. Micromech. Microeng.* **9** 194–8

[5] Venstra W J and Sarro P M 2003 Fabrication of crystalline membranes oriented in the (1 1 1) plane in a (1 0 0) silicon wafer *Microelectron. Eng.* **67–68** 502–7

[6] Sasaki M, Yamaguchi T, Song J H, Hane K, Hara M and Hori K 2003 Optical scanner on a three-dimensional microoptical bench *J. Lightwave Technol.* **21** 602–8

[7] Pal P and Chandra S 2004 Bulk-micromachined structures inside anisotropically etched cavities *Smart Mater. Struct.* **13** 1424–9

[8] Venstra W J, Pham N P, Sarro P M and van Eijk J 2005 Particle filters integrated inside a silicon wafer *Microelectron. Eng.* **78–79** 138–41

[9] Yue M, Lin H, Dedrick D E, Satyanarayana S, Majumdar A, Bedekar A S, Jenkins J W and Sundaram S 2004 A 2-d microcantilever array for multiplexed biomolecular analysis *J. Microelectromech. Syst.* **13** 290–9

[10] Kutchoukow V G, Mollinger J R and Bossche A 1999 Novel method for spinning of photoresist on wafers with through-hole *Proc. 13th European Conf. on Solid-State Transducers (Eurosensors)* pp 256–72

[11] Luxbacher T and Mirza A 1999 Spraycoating for MEMS, interconnect & advanced packaging applications *HDI Mag.* 36–41

[12] Wieder B, Brubaker C, Glinsner T, Kettner P and Nodes N 2002 Spraycoating for MEMS, NEMS and microsystems

Pacific RIM workshop on Transducers and Micro/Nanotechnologies

[13] Singh V K, Sasaki M, Hane K and Esashi M 2004 Flow condition in resist spray coating and patterning performance for three-dimensional photolithography over deep structures *Japan. J. Appl. Phys.* **43** 2387–91

[14] Kersten P, Bouwstra S and Petersen J W 1995 Photolithography on micromachined 3d surfaces using electrodeposited photoresists *Sensors Actuators* A **51** 51–4

[15] Pham N P, Boellaard E, Burghartz J N and Sarro P M 2004 Photoresist coating methods for the integration of novel 3-d rf microstructures *J. Microelectromech. Syst.* **13** 491–9

[16] Pham N P, Burghartz J N and Sarro P M 2005 Spray coating of photoresist for pattern transfer on high topography surfaces *J. Micromech. Microeng.* **15** 691–7

[17] Alamir A S A 2003 On the rotation-free and distortion-free systems *Optik* **114** 509–13

[18] Electronic Visions Co. 1998 Operation Manual EV420: Double Side Mask Aligner